

The influence of areal density of prepreg on crashworthiness of CFRP composite in quasi-static conditions

Grażyna Rzyńska

Rzeszow University of Technology, Aleja Powstańców Warszawy 8, 35-029 Rzeszów, Poland

e-mail: grar@prz.edu.pl

<https://doi.org/10.62753/ctp.2025.02.2.2>

Abstract: In this work, experimental compression tests were performed in quasi-static conditions on composite specimens in the form of tubes of two different diameters (20 mm and 42 mm). The specimens were made of 3k carbon prepregs with a dry fabric areal density of 160 g/m² and 204 g/m², plain, and unidirectional (UD) with an areal density of 200 g/m². The experiment determined the maximum forces (P_{max}), average forces (P_i), and the value of absorbed energy (SEA). It was shown that the use of a 21% higher areal density increases the SEA by about 25% for the plain prepreg. Changing the type of prepreg from plain to UD with a similar areal density increases the SEA by 39% - 53%.

Keywords: CFRP, composite, crushing, SEA, areal density

1. Introduction

The production of increasingly lighter vehicles is currently a determinant of the development of the automotive, aviation and rail industries. Composites of various compositions are widely used as materials not only for construction but also as visually attractive elements of vehicle interior fittings. Progressively more metal elements are being replaced with composite products. Undoubtedly, a major advantage of composite materials is their low specific weight, which provides great economic benefits related to reduced fuel consumption. In addition, selected composite materials are characterized by high durability. Another feature of selected composite materials is their ability to absorb large amounts of energy in the process of controlled destruction. This is a premise for designing lightweight structures as equivalents of steel elements absorbing impact energy. Such a material is, among others, a carbon fiber reinforced epoxy composite [1-5]. The advantages of this type of material include excellent mechanical properties, low density, high strength and specific stiffness, as well as a promising potential for effective vibration control and noise reduction [6].

When analyzing the results presented by researchers, it should be noted that carbon fibers used in an appropriate geometric arrangement reinforced with epoxy resin can give very good results at the level

of 120 kJ/kg [7, 8]. The specific properties of epoxy composites reinforced with carbon fabric mean that they can be used to design elements that will absorb more energy than metal elements or composites reinforced with glass fiber [3, 5, 8, 9, 10, 11]. The basic criterion for the operation of such an element is to absorb energy in a gradual and controlled manner because the main goal is the safety of transported goods and people.

2. Factors affecting the amount of energy absorbed

The factors that influence the absorption of impact energy are: structural, technological, geometrical and test conditions-dependent factors [12]. In addition, the type of material and the type of cross-section geometry, wall thickness to diameter, type of load and composite architecture have an impact [3, 13, 14, 15, 16, 17, 18]. A significant role in energy absorption is played by friction, in particular friction between the profile and the initiator, as proven in [19]. In general, the properties of composite materials reinforced with long fibers grow with the increase in the fiber content [20, 21], but the effect of the fiber content in the composite on the ability to absorb energy is not clear. The course of the crushing process of composite profiles is related to the material properties of the composite, which result from many factors such as the mechanical properties of the fiber and resin, the laminate structure and fiber content [12, 22]. Nevertheless, in this approach, the effect of the fiber content on the energy absorption capacity of composite structures has not been studied in detail. Some authors found that a decrease in the SEA value is observed with the increase in the volume content of fibers [22, 23, 24]; others found that increasing the fiber content causes an rise in SEA [10, 25, 26]. Although the conclusions of various authors are not consistent, it should be taken into account that the influence of the fiber content on the ability to absorb impact energy may be different for various materials and for different analyzed ranges of fiber volume fractions in the composite. Nonetheless, since SEA changes are related to phenomena occurring between laminate layers [27], the influence of the fiber content on the parameters describing these phenomena should be considered. On the other hand, with the increase in the fiber content, the volume of the matrix between the fibers decreases, changing the density of the material. This is all the more important with the greater the difference between the density of the matrix material and the density of the fibers. In papers [3, 12, 28, 29] it was proven that the fiber orientation ± 45 absorbs significantly less energy compared to the [0/90] arrangement and random reinforcement with a mat [30]. Among the factors influencing SEA, the areal density of the reinforcement used is also worth noting, however, there are not many studies of this type. In study [32] 30%-52% ILLS was found for the areal density of 380 g/m² compared to the areal density of 200 g/m². In work [33], static and dynamic tests were carried out on round specimens of 20 mm in diameter with an areal density of 160 g/m². It was shown that SEA in static conditions was 65 J/g and in dynamic conditions 48 J/g. In work

[8] quasi static and dynamic compression tests were performed on specimens 42 mm in diameter reinforced with a fabric of 204 g/m². The obtained SEA was 85.47 J/g for quasi-static conditions and 67.97 J/g for dynamic conditions. Studies [7] showed the occurrence of the scale effect, i.e. a higher SEA was obtained for smaller specimens compared to specimens of a larger diameter.

Taking the above into account, the present studies were carried out to assess the effect of the composite fiber arrangement and the areal density of the used prepreg on the amount of absorbed energy during its crushing in quasi-static conditions on specimens of two different diameters.

3. Materials and methods

3.1. Materials

In order to perform experimental studies aimed at investigating the influence of selected factors on SEA, a number of composite pipes with a given architecture were made. For this purpose, three types of prepregs (3k) carbon fiber-epoxy resin (IMP 503Z40) from Impregnatex Compositi (Fig. 1) were used, with properties determined experimentally in accordance with ASTM standards [34-36] and presented in Table 1.



Fig. 1. Prepregs used in tests, a) UD 200g/m², b) plain 160 g/m², c) plain 204 g/m²

Table 1. Properties of tested materials. Tests were performed in accordance with ASTM standards

Parameter	204 3k	160 3k	200 UD
Areal density, g/m ²	204	160	200
Resin content, %	47	47	47
Type of resin	IMP 503Z40	IMP 503Z40	IMP 503Z40
E _{1t} , MPa	50 439.53	52 748.09	104 634.0
E _{2t} , MPa	49 888.38	51 134.81	9 914.0
σ _{1t} , MPa	654.67	500.81	1 723.0
σ _{2t} , MPa	679.12	439.28	78.58
ε _{1t} , %	1.23	1.05	1.48
ε _{2t} , %	1.27	0.82	0.81
GI (Mode I), J/m ²	CC 368.745	CC 220.37	CC 340.793
GII (Mode II), J/m ²	NPC 2234.173 PC 2412.167	NPC 1833.48 PC 1189.28	NPC 2263.70 PC 2316.26

Pipes 0.5 m long were made by manually winding layers of the appropriate prepreg onto a Teflon core of the appropriate diameter. Teflon cores with diameters of 42 mm and 20 mm were used. The specimen designations were introduced in accordance with Table 2. Curing was carried out in an autoclave at 130°C for three hours. Then the pipes were cut into specimens of the appropriate length (Fig. 2.).

Table 2. Test specimen parameters

Designation	Diameter, mm	Number of prepreg layers	Areal density, g/m ²	Type of prepreg
I	42	10	200	UD
II	42	10	204	plain
III	42	10	160	plain
IV	20	5	204	plain
V	20	5	200	UD
VI	20	5	160	plain

To reduce the crushing initiation force of the composite pipes, each specimen was finished with a single-sided external chamfer of 70° (Fig. 2.).

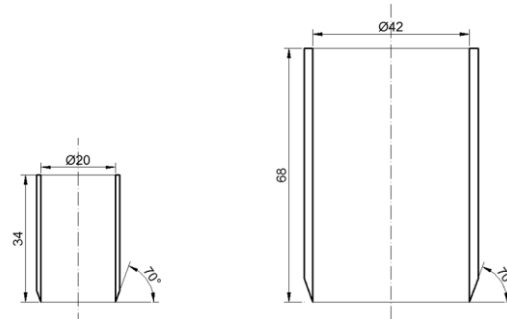


Fig. 2. Geometry of specimens (units are given in millimeters)

3.2. Procedure for determining the energy absorbed by a unit mass (SEA)

To calculate the absorbed energy per unit mass (SEA), one needs to determine: the total energy absorbed by the specimen during the test, the specimen density, and the cross-sectional area of each specimen.

SEA can be calculated using the formula:

$$SEA = \frac{E_{tot}}{\rho Al} \quad (1)$$

E_{tot} – total energy absorbed in the test, ρ – average density, A – cross-sectional area, l – displacement

The total energy absorbed in the test was determined by calculating the area under the force-displacement graph obtained in the crush test of the composite specimens. The density was determined experimentally. The average results of nine measurements for each specimen are presented in Table 3.

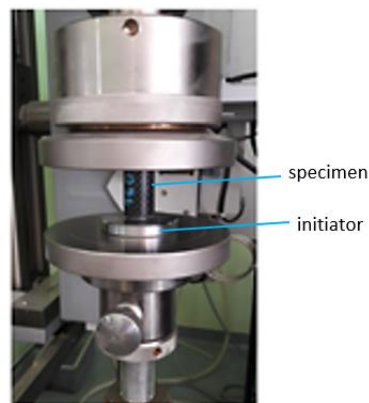
Table 3. Density and cross-sectional area for tested variants of composite specimens

Designation	Density, g/cm ³	A, mm ²
I	1.562	305.33
II	1.453	319.93
III	1.415	276.32
VI	1.415	65.94
V	1.562	72.88
IV	1.453	76.37

4. Research and discussion

4.1. The influence of areal density and architecture on SEA

Quasi-static crushing tests for the specimens with the diameter of 42 mm were carried out using a Zwick 100 kN universal testing machine, while tests for the specimens with the diameter of 20 mm were carried out by means of a Zwick 30 kN universal testing machine. The test stand is shown in Figure 3. Three specimens were tested for each case at a constant speed of $v=0.0003$ m/s. For the specimens with the diameter of 42 mm, displacements of 55 mm were set, while for the specimens with the diameter of 20 mm, a displacement of 25 mm was set. An initiator with a working edge radius of $r=1$ mm was used in the tests.

**Fig. 3. Stand for testing in quasi-static conditions for 20 mm diameter specimens; testing velocity $v=20$ mm/min**

As a result of the experimental tests, force-displacement curves were obtained for all the tested specimen variants (Fig. 4, 7). The appearance of the specimens after the test is shown in the figures (Fig. 5, 8).

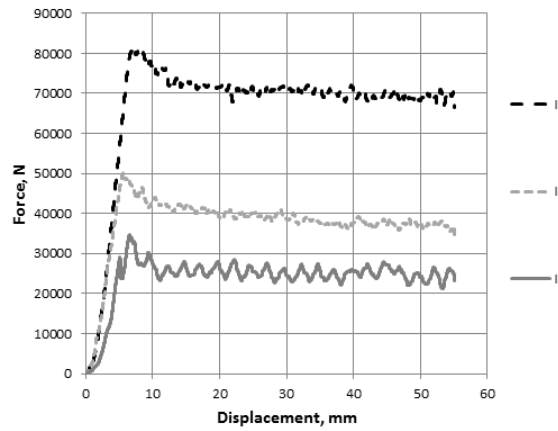


Fig. 4. Force-displacement curves, 42 mm diameter specimens, tests velocity $v=20$ mm/min; comparison of type I, II and III specimens

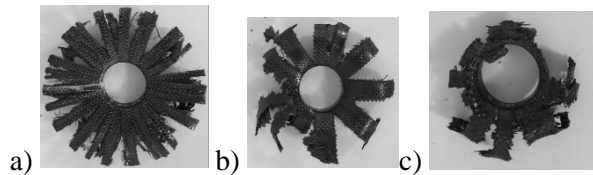


Fig. 5. Example 42 mm diameter specimens after testing; a) specimen type I; b) II; c) III

The calculated mean SEA values for all the specimen types are presented in graphs (Fig. 6, 9).

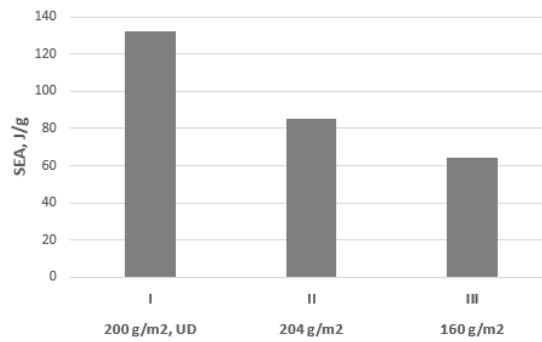


Fig. 6. SEA for 42 mm diameter specimens

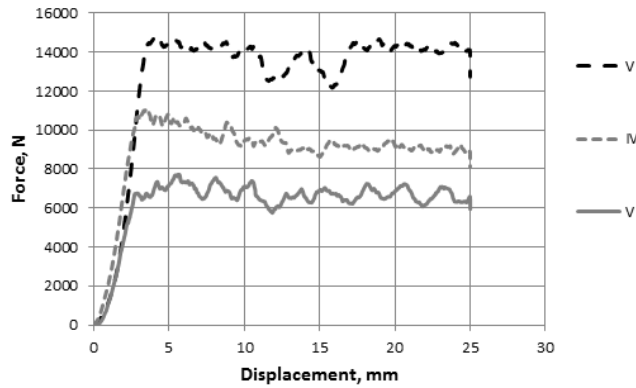


Fig. 7. Force-displacement curves, 20 mm diameter specimens, test velocity $v=20$ mm/min; comparison of type V, IV and VI specimens

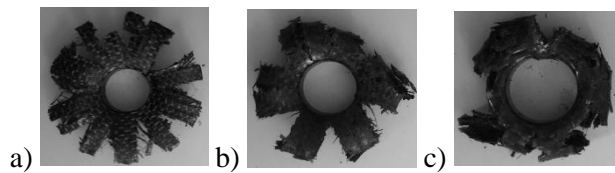


Fig. 8. Example 20 mm diameter specimens after testing; a) specimen type V; b) IV; c) VI;

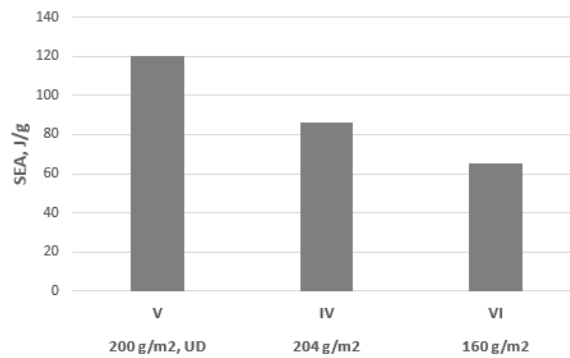


Fig. 9. SEA for 20 mm diameter specimens

The value of average force P_1 (which was determined as the average value of force after the crushing process had started) in relation to maximum force P_{max} for all the specimen types is presented in Table 4. The P_i/P_{max} value shows the effectiveness of the initiator in the process, which is to reduce the P_{max} force. Table 4 shows different P_i/P_{max} values, which indicate the need to select an individual initiator for the specimen type.

Table 4. P_i/P_{max} values for series of 20 mm and 42 mm diameter specimens

Designation	P_i/P_{max}
I	0.76±0.11
II	0.76±0.11
III	0.73±0.01
IV	0.89±0.03
V	0.92±0.03
VI	0.85±0.03

When analyzing the results of the crushing tests of the composite specimens in quasi-static conditions, attention is drawn to the force-displacement curve, the courses of which are uniform, which is very beneficial regarding energy absorption. Small fluctuations were observed in the case of the specimens from group III, where the force oscillates in the entire displacement range. The most stable courses were observed in the case of the specimens containing only axial fibers for both tested diameters (I, V), which may be due to the lack of the effect of cracking of peripheral fibers causing force fluctuations. The appearance of the specimens after the quasi-static tests indicates the occurrence of a delamination mechanism in the case of a larger share of axial fibers; for a smaller share of axial fibers, more intensive fiber crumbling and a decreasing number of axial cracks can be observed, which indicates the predominance of the fragmentation mechanism. In order to show the changes in SEA caused by the change of the material used, the results for the type VI specimens together with the type IV specimens crushed in quasi-static conditions, and the type III specimens together with the type II specimens crushed also in quasi-static conditions were compared (Tables 5, 6). A change in the areal density by 21.5% causes a rise in SEA by about 25%.

Table 5. Influence of areal density of prepreg and density of finished composite on obtained values of force and SEA in process of crushing type IV and VI composite specimens in quasi-static conditions

Designation	Areal density, g/m^2	Density, g/cm^3	P_i , N	P_{max} , N	SEA, J/g
VI	160	1.415	7125.49	8378.10	65.14
IV	204	1.453	9492.12	11096.54	86.81
Difference %	21.56	2.61	24.93	24.49	24.96

Table 6. Influence of areal density of prepreg and density of finished composite on obtained values of force and SEA in process of crushing type II and III composite specimens in quasi-static conditions

Designation	Areal density, g/m ²	Density, g/cm ³	P _i , N	P _{max} , N	SEA, J/g
III	160	1.415	27409.02	37350.04	64.38
II	204	1.453	41135.01	52402.49	86.37
Difference %	21.56	2.61	33.36	28.72	25.45

Tables 7 and 8 additionally present the difference in the obtained force and SEA for specimens made of UD and plain prepreps. The introduction of the UD prepreg in both cases of the tested diameters compared to a similar areal density plain prepreg increases the SEA by 39% for the small specimens and 53% for the specimens with the larger diameter.

Table 7. Influence of areal density of prepreg and density of finished composite on obtained values of force and SEA in process of crushing type V and IV composite specimens in quasi-static conditions

Designation	Areal density, g/m ²	Density, g/cm ³	P _i , N	P _{max} , N	SEA, J/g
V	200	1.562	13847.31	14918.61	120.70
IV	204	1.453	9492.12	11096.54	86.81
Difference %	1.96	7.50	45.88	34.44	39.03

Table 8. Influence of areal density of prepreg and density of finished composite on obtained values of force and SEA in process of crushing type I and II composite specimens in quasi-static conditions

Designation	Areal density, g/m ²	Density, g/cm ³	P _i , N	P _{max} , N	SEA, J/g
I	200	1.562	64861.82	85279.86	132.14
II	204	1.453	41135.01	52402.49	86.37
Difference %	1.96	7.50	57.68	62.74	52.97

5. Conclusions

1. A change in the areal density by 21% with the same reinforcement type (with an axial fiber content of 50%) causes an increase in SEA for the quasi-static test by about 25%.
2. The content of axial fibers has a significant influence on both the maximum forces, average force, and consequently, on the amount of energy absorbed in the compression process of the composite specimens.

3. The performed tests have shown that increasing the share of axial fibers from 50% to 100% raises the amount of absorbed energy for the quasi-static test by 39 - 53%.
4. The applied constant trigger angle allowed the initial force in the process to be reduced, but significant differences were observed depending on the axial fiber content, which indicates the need to select the trigger geometry depending on the architecture of the composite element.

References:

1. Farley G.L., The effect of crushing speed on the energy – absorption capability of composite tubes, *Journal of Composite Materials* 1991, 25, 1314-1329, <https://doi.org/10.1177/002199839102501004>.
2. Farley G.L., Jones R.M., Crushing characteristic of continuous fiber-reinforced composite tubes, *Journal of Composite Materials* 1992, 26, 37-50, <https://doi.org/10.1177/002199839202600103>.
3. Hull D., A unified approach to progressive crushing of fibre-reinforced composite tubes, *Composites Science and Technology* 1991, 40, 377–421, [https://doi.org/10.1016/0266-3538\(91\)90031-J](https://doi.org/10.1016/0266-3538(91)90031-J).
4. Mahdi E., Sahari B., Hamouda A., Khalid Y., An experimental investigation into crushing behavior of filament-wound laminated cone-cone intersection composite shell, *Composite Structures* 2001, 51, 211-219, [https://doi.org/10.1016/S0263-8223\(00\)00132-X](https://doi.org/10.1016/S0263-8223(00)00132-X).
5. Mamalis A., Manolakos D., Ioannidis M., Papapostolou D., On the experimental investigation of crash energy absorption in laminate splaying collapse mode of FRP tubular components, *Composite Structures* 2005, 70, 413–429, <https://doi.org/10.1016/j.compstruct.2004.09.002>.
6. Isaac A., Pawelczyk C.W., M., Wrona, S., Comparative study of sound transmission losses of sandwich composite double panel walls, *Appl. Sci.* 2020, 10, 1543, <https://doi.org/10.3390/app10041543>.
7. Rzyńska G., Gieleta R., Experimental studies on impact of CFRP tubes structure on amount of absorbed energy under dynamic conditions, *Composites Theory and Practice* 2018, 18, 4, 196-201.
8. Rzyńska G., David M., Prusty G., Tarasiuk J., Wroński S., Effect of fibre architecture on the specific energy absorption in carbon epoxy composite tubes under progressive crushing, *Composite Structures* 2019, 227, 2019, 111292, <https://doi.org/10.1016/j.compstruct.2019.111292>.
9. Huang X., Lu G., Yu T.X., Energy absorption in splitting square metal tubes, *Thin-Walled Structures* 2002, 40, 153–165, [https://doi.org/10.1016/S0263-8231\(01\)00058-1](https://doi.org/10.1016/S0263-8231(01)00058-1).
10. Ramakrishna S., Hamada H., Energy absorption of crash worthy structural composite materials, *Key Engineering Materials* 1998, 141-143, 585-622, [10.4028/www.scientific.net/KEM.141-143.585](https://www.scientific.net/KEM.141-143.585).
11. Farley G.L., Jones R.M., Crushing characteristic of continuous fiber-reinforced composite tubes, *J Compos Mater* 1992, 26, 1, 37-50, <https://doi.org/10.1177/002199839202600103>.
12. Ramakrishna S., Microstructural design of composite materials for crashworthy structural applications, *Material & Design* 1997, 18, 167–173, [https://doi.org/10.1016/S0261-3069\(97\)00098-8](https://doi.org/10.1016/S0261-3069(97)00098-8).
13. Alkoles O.M.S., Mahdi E., Hamouda A.M.S., Sahari B.B., Ellipticity ratio effects in the energy absorption of axially crushed composite tubes, *Applied Composite Materials* 2003, 10, 339–363, [10.1023/A:1025766609635](https://doi.org/10.1023/A:1025766609635).
14. Czaplicki M., Robertson R., Thornton P., Comparison of bevel and tulip triggered pultruded tubes for energy absorption, *Composites Science and Technology* 1991, 40, 31-46, [https://doi.org/10.1016/0266-3538\(91\)90041-M](https://doi.org/10.1016/0266-3538(91)90041-M).

15. Farley G., Effect of fiber and matrix maximum strain on the energy absorption of composite materials, *Journal of Composite Materials* 1986, 20, 322-334, 10.1177/002199838602000401.
16. Farley G.L., Effect of specimen geometry on the energy absorption capability of composite materials, *Journal of Composite Materials* 1986, 20, 390-400, <http://dx.doi.org/10.1177/002199838602000406>.
17. Gupta N., Velmurugan R., Gupta S., An analysis of axial crushing of composite tubes, *Journal of Composite Materials* 1997, 31, 1262–1286, 10.1177/002199839703101301.
18. David M., Johnson A., Voggenreiter H., Analysis of crushing response of composite crashworthy structures, *Applied Composite Materials* 2013, 20, 773–787, 10.1007/s10443-012-9301-8.
19. Swaminathan N., Averill R. C., Contribution of failure mechanisms to crush energy absorption in a composite tube, *Mechanics of Advanced Materials and Structures* 2006, 13, 1, 51–59, <https://doi.org/10.1080/15376490500343782>.
20. Ochlewski S., *Metody doświadczalne mechaniki kompozytów konstrukcyjnych*, WNT – Warszawa 2004.
21. Lavoie J.A., Kellas S., Dynamic crush tests of energy-absorbing laminated composite plates, *Composites Part A* 1996, 27, 467–75.
22. Ramakrishna S., Hull D., Energy absorption capability of epoxy composite tubes with knitted carbon fibre fabric reinforcement, *Composite Science and Technology* 1993, 49, 349-356, [https://doi.org/10.1016/0266-3538\(93\)90066-P](https://doi.org/10.1016/0266-3538(93)90066-P).
23. Jacob G., Fellers J., Simunovic S., Starbuck J., Energy absorption in polymer composites for automotive crashworthiness, *Journal of Composite Materials* 2002, 36, 813–850, <https://doi.org/10.1177/0021998302036007164>.
24. Farley G.L., Energy absorption of composite material and structures, In: *Proceedings of 43rd American Helicopter Society annual forum*, St. Louis, USA, 1987, 613-27.
25. Snowdon P., Hull D., Energy absorption of SMC under crash conditions, In: *Proceedings of fiber reinforced composites conference '84*. Plastics and Rubber Institute, 1984, 5.1-5.10.
26. Thornton P.H., Tao W.H., Robertson R.E., Crash energy management: axial crush of unidirectional fiber composite rods, *Advanced Composite Materials: New Developments and Applications*, 1991, 489-496.
27. Daniel L., Hogg P.J., Curtis P.T., The crush behavior of carbon fiber angle-ply reinforcement and the effect of interlaminar shear strength on energy absorption capability, *Composites Part B* 2000, 31, 435-40, 10.1016/S1359-8368(00)00026-3.
28. Pickett L., Dayal V., Effect of tube geometry and ply-angle on energy absorption of a circular glass/epoxy crush tube – a numerical study, *Composites Part B: Eng* 2012, 43, 2960–2967, 10.1016/j.compositesb.2012.05.040.
29. Thornton P. H., Energy absorption in composite structures, *Journal of Composite Materials* 1979, 13, 247-262, <https://doi.org/10.1177/002199837901300308>.
30. Warrior N.A., Turner T.A., Robitaille F., Rudd C.D., Effect of resin properties and processing parameters on crash energy absorbing composite structures made by RTM, *Composites Part A* 2003, 34, 543-550, [https://doi.org/10.1016/S1359-835X\(03\)00057-5](https://doi.org/10.1016/S1359-835X(03)00057-5).
31. Kim Jung-Seok, Yoon Hyuk-Jin, Shin Kwang-Bok, A study on crushing behaviors of composite circular tubes with different reinforcing fibers, *International Journal of Impact Engineering* 2011, 38, 198-207, 10.1016/j.ijimpeng.2010.11.007.
32. Biswas R., Sharma N., Singh K. K., Influence of fiber areal density on mechanical behavior of basalt fiber/epoxy composites under varying loading rates: An experimental and statistical approach, *Polymer Composites* 2023, 44, 4, 2222, <https://doi.org/10.1002/pc.27238>.
33. Rzyńska G., Gieleta R., Effect of test velocity on the specific energy absorption under progressive crushing of composite tubes, *Advances in Science and Technology Research Journal* 2020, 14, 2, 94–102, <https://doi.org/10.12913/22998624/118551>.

34. ASTM D3039/D3039M Standard Test Method for Tensile Properties of Polymer Matrix Composite Materials, 2008.
35. ASTM D7905 / D7905M – 14, Standard Test Method for Determination of the Mode II Interlaminar Fracture Toughness of Unidirectional Fiber-Reinforced Polymer Matrix Composites.
36. 55ASTM D5528 Standard Test Method for Mode I Interlaminar Fracture Toughness of Unidirectional Fiber-Reinforced Polymer Matrix Composites.